文章编号:1671-4229(2024)01-0029-09

利用溶液加工的界面阻挡层实现高效三维和准二维金属卤化物钙钛矿发光二极管

王林强[1a],贾亚兰[2],徐 强[2],朱志新[2],
周科文[1a],高春红[1a,1b,1c,2*],潘书生[1a,1b,1c**]

(1. 广州大学 a. 物理与材料科学学院, b. 硅基信息材料与集成电路设计广东普通高校重点实验室, 广东 广州 510006, c. 黄埔研究院研究生院先进信息材料研究中心, 广东 广州 510555; 2. 西南大学 物理科学与技术学院, 重庆 400715)

摘 要: 为了保护金属卤化物钙钛矿发光层免受强酸性聚合物(poly-(3,4-ethylenedioxythiophene):poly(styrenesulfonic acid),PEDOT:PSS)的腐蚀,一种具有空穴传输能力的有机小分子材料(N,N-dicarbazolyl-3,5-benzene,mCP)被当作界面阻挡层引入三维钙钛矿发光层($CsPbBr_3$)和PEDOT:PSS之间。研究表明,mCP不仅可以从空间上隔离$CsPbBr_3$和PEDOT:PSS,抑制PEDOT:PSS对$CsPbBr_3$发光层的降解,还可以使钙钛矿薄膜的覆盖率更高,颗粒更小,提高薄膜质量,减少薄膜缺陷对激子的淬灭。同时,mCP的引入可以提高空穴注入和传输能力,使得相同电压下形成的激子更多;由于mCP具有比PEDOT:PSS更高的最低电子不占有态和更大的能隙,能更好地将激子限制在发光层中,进一步提高激子的发光辐射复合和器件的电致发光效率。与原始不加mCP的器件相比,基于mCP的3D $CsPbBr_3$钙钛矿发光二极管(Perovskite light-emitting diode,PeLED)的电致发光性能得到了显著提升,获得了4.86 cd/A最大电流效率。接着,这种方法在基于$PEA_2Cs_{n-1}Pb_nBr_{3n+1}$的准二维PeLED中也被证实是可行的,器件的最大电流效率被提升到24.79 cd/A。

关键词: 激子阻挡; 空穴传输; 电致发光; 钙钛矿发光二极管

中图分类号: TN312.8;TB34 **文献标志码**: A

Efficient 3D and quasi-2D metal halide perovskite light-emitting diodes by a solution processed interface barrier layer

WANG Lin-qiang[1a], *JIA Ya-lan*[2], *XU Qiang*[2], *ZHU Zhi-xin*[2], *ZHOU Ke-wen*[1a],
GAO Chun-hong[1a,1b,1c,2*], *PAN Shu-sheng*[1a,1b,1c**]

(1. a. School of Physics and Materials Science, b. Key Laboratory of Si-Based Information Materials & Devices and Integrated Circuits Design of Guangdong Higher Education Institutes, Guangzhou University, Guangzhou 510006, China, c. Research Center for Advanced Information Materials (CAIM), Huangpu Research & Graduate School of Guangzhou University, Guangzhou 510555, China; 2. School of Physical Science and Technology, Southwest University, Chongqing 400715, China)

Abstract: An organic small molecular material (N,N-dicarbazolyl-3,5-benzene, mCP) with hole transporting

Received date: 2023-07-12 **Revised date**: 2023-12-06

Foundation items: Key Discipline of Materials Science and Engineering, Bureau of Education of Guangzhou (No. 202255464); "2+5" Significant Academic Hubs and Platforms of Guangzhou University (PT252022016)

Biography: WANG Lin-qiang (1990—), male, graduate student. E-mail:2112119020@e.gzhu.edu.cn

* Corresponding author. E-mail:gch0122@gzhu.edu.cn

** Corresponding author. E-mail:sspan@gzhu.edu.cn

Citation: WANG L Q, JIA Y L, XU Q, et al. Efficient 3D and quasi-2D metal halide perovskite light-emitting diodes by a solution processed interface barrier layer[J]. Journal of Guangzhou University(Natural Science Edition),2024,23(1):29-37.

ability was introduced as an interfacial barrier layer between the metal halide perovskite luminescent layer ($CsPbBr_3$) and the strongly acidic polymer poly-(3,4-ethylenedioxythiophene):poly(styrenesulfonic acid) (PEDOT:PSS) to protect $CsPbBr_3$ from corrosion. The study showed that mCP not only can spatially isolate $CsPbBr_3$ and PEDOT:PSS to inhibit the degradation of PEDOT:PSS on the $CsPbBr_3$ luminescent layer, but also can improve the film quality, making the coverage of the perovskite film higher and the grains smaller, and thus reducing the quenching defect. At the same time, the introduction of mCP can improve the hole injection and transport ability, resulting in more excitons generated under the same voltage. Since mCP has a higher lowest electron unoccupied state and a larger energy gap than PEDOT:PSS, which can confine excitons better in the luminescent layer, improving the radiation recombination of excitons, thereby improving the electroluminescence efficiency of the device further. Compared with the reference device without mCP, the electroluminescence performance of the 3D $CsPbBr_3$ perovskite light-emitting diode (PeLED) based on mCP was significantly improved, achieving a maximum current efficiency of 4.86 cd/A. Subsequently, this method was also proven to be feasible in quasi-two-dimensional PeLEDs based on $PEA_2Cs_{n-1}Pb_nBr_{3n+1}$, exhibiting the maximum current efficiency of 24.79 cd/A.

Key words: exciton blocking; hole transport; electroluminescence; perovskite light-emitting diode

1 Introduction

Metal halide perovskites are widely applied in light-emitting diodes (LEDs), since the first room temperature perovskite light-emiting diode (PeLEDs) was achieved in 2014[1]. Although the external quantum efficiency (EQE) of the first reported room temperature PeLEDs was only 0.1%, it was above 10% for pure blue, exceeding 30% for green, and surpassing 20% for red and near infrared ones till now[2-8]. And they have been recognized as a new type of emitters in the field of lighting and display due to their excellent photoelectric properties, such as long exciton diffusion length, high carrier mobility, tunable optical band gap and high photoluminescence quantum efficiency (PLQY)[9-12]. In addition, they are low cost and can be easily prepared by a simple solution treatment. However, the efficiency and the stability are not good enough for their commercialization.

Recently, poly-(3,4-ethylenedioxythiophene):poly(styrenesulfonic acid) (PEDOT:PSS) is the most commonly used hole injection and transporting layer in PeLEDs due to its high conductivity and high transparency[13-25]. It is often adjacent to the metal halide perovskite light-emitting layer (EML). The perovskite EML may be degraded by PEDOT:PSS, since it is a strong acid with a pH value of 1 to 2[13]. Moreover, the excitons generated at the interface of PEDOT:PSS/perovskite EML may be quenched by PEDOT:PSS. Two reasons should be considered. One reason may be attributed to the small energy gap (E_g) of PEDOT:PSS (3.0 eV)[14], which is not large enough to confine excitons in the perovskite EML. The other reason should be due to the fact that the holes on the highest occupied molecular orbital (HOMO) of PEDOT:PSS (−5.2 eV)[15] and electrons on the conducting band (CB) of the $CsPbBr_3$ (−3.35 eV)[16] may be quenched via non-radiation and produce joule heat, which may further do harm to the stability of the PeLEDs.

To solve the above problems, kinds of methods are developed. Doping engineering and interface barrier layer method are two wildly used methods. In doping engineering, polymers, inorganic materials and base materials are involved. Polymers are brought in to make the HOMO lower, e.g. tetrafluoroethylene-perfluoro-3, 6-dioxa-4-methyl-7-octene-sulfonic acid copolymer (PFI)[17], sodium-poly(styrenesulfonate) (S-PSS)[18]. To neutralize the acidic nature of PE-

DOT:PSS and protect perovskite EML from etching, base materials are used including NaOH[19] or imidazole[20]. The MoO_3-Ammonia:PEDOT:PSS blending is utilized, aiming to reduce the HOMO and neutralize the acidic nature[21]. While for the interface barrier layer method, polymers are the most common used buffer layer to isolate PEDOT:PSS and perovskte, for example poly(9,9-di-n-octylfluorenyl-2,7-diyl) (PFO)[22], poly[(9,9-bis(3′-(N,N-dimethylamino) propyl)-2,7-fluorene)-alt-2,7-(9,9-dioctylfluorene)] (PFN)[23]. However, there are only a few reports on the solution processed small organic molecule interface buffer layer, due to their low solubility in non-polar organic solvents. The organic small molecule, named triphenylphosphine oxide (TPPO), is brought between the HTL and perovskite layer. The lone pair electrons of P = O in it can passivate the defects in perovskite and help the PeLEDs obtain a maximum external quantum efficiency (EQE_{max}) of 21.01%[24]. In our group's previous work, a solution process small organic molecule, named 4,4′-cyclohexylidenebis[N,N-bis(p-tolyl) aniline] (TAPC), was demonstrated in the 3D $CsPbBr_3$ PeLEDs showing an improved efficiency with a EQE of 1.77%[25]. The low EQE should be attributed to the high HOMO of TAPC (−5.5 eV)[26], which may cause that the holes on HOMO of TAPC (−5.5 eV) and the electron on the CB of $CsPbBr_3$ to be quenched via non-radiation and produce joule heat, and do harm to the PeLEDs. To solve this problem, a small organic molecule N,N-dicarbazolyl-3,5-benzene (mCP) was chosen to be an interface barrier layer for PEDOT:PSS degradation and exciton quenching. The EL performance of 3D $CsPbBr_3$ perovskite light-emitting diode (PeLED) based on mCP was significantly improved, exhibiting the maximum current efficiency of 4.86 cd/A and the maximum luminance of 14 247 cd/m^2. And the interface barrier behaviors of mCP are further confirmed in the quasi-2D $PEA_2Cs_{n-1}Pb_nBr_{3n+1}$ PeLEDs, exhibiting a maximum EQE of 6.52% with a maximum luminance of 28 438 cd/m^2.

2　Experiment and measurement

2.1　Materials and solutions

Materials: CsBr (99.999%) was bought from Alfa Aesar. $PbBr_2$ (>99.99%) and 2-phenylethanamine bromide (PEABr, >99.5%) was purchased from Xi'an Polymer Light Technology Corp. Anhydrous dimethyl sulfoxide (DMSO, >99.9%) and chlorobenzene (99.8%) were obtained from Sigma Aldrich. 1,3-bis(9-carbazolyl) benzene (mCP, >99%) was acquired from Suzhou Fangsheng Photoelectricity Shares Co., Ltd.

The mCP solution is achieved by dissolving mCP in chlorobenzene at 8 mg/ml. The 10 wt.% $CsPbBr_3$ perovskite precursor is prepared by stirring both CsBr and $PbBr_2$ with a mole ratio of 1∶1.2 for more than 12 h. The quasi-2D $PEA_2Cs_{n-1}Pb_nBr_{3n+1}$ perovskite precursor that was prepared by employing $PbBr_2$, CsBr and PEABr was dissolved in anhydrous DMSO with molar ratio of 1∶1∶0.4 at a concentration of 0.2 M. All of the above solutions were prepared in glove box at room temperature.

2.2　Device fabrication

PeLEDs were fabricated on indium tin oxide (ITO, 15 Ω sq^{-1}) glass substrates. The ITO substrates were firstly ultrasonic cleaned in deionized water, ethanol and acetone for 15 min successively. Secondly, they were dried in an oven at 100 ℃ for 20 min. At last, they were UV-ozoned (SunMonde-UVO3 Clearner-120W) for 5 min to reduce the work function of ITO to −4.7 eV.[15] The PEDOT:PSS layer was deposited on a clean ITO by spincoating PEDOT:PSS solution at 4500 rpm for 40 s and then dried by a hotplate in air at 100 ℃ for 20 min to remove the water. The samples were pumped away in a vacuum chamber at −1.0 bar for 30 min and then transferred into the glovebox. mCP solutions, 10 wt.% $CsPbBr_3$ precursors and/or $PEA_2Cs_{n-1}Pb_nBr_{3n+1}$ perovskite precursors were spincoated on PEDOT:PSS successively at 4 000 rpm for 60 s. For each spincoated film, they were pumped away in the transfer chamber for 20 min to remove the solvent.

And then, the samples were transferred into a thermal deposition chamber (Shenyang Vacuum Technology Research Institute) (5×10^{-4} Pa) to sequentially deposit layers of TmPyPB (65 nm), Liq (2 nm), and Al (150 nm) at rates of 1 Å/s, 0.1 Å/s, 2 Å/s, respectively. Finally, all the devices were sealed with glass covers in a nitrogen-filled glove box. The electroluminescence (EL) performances of PeLEDs were tested in ambient air. The active area of the device depending on the deposition mask was 6 mm^2.

2.3 Measurements and characterizations

The top-view of the perovskite films were scanned by scanning electron microscope (SEM, JEOL JSM-7100F). The X-ray diffractometer (XRD) patterns were measured by XRD, TD-3500. UV-Vis absorption spectra were carried by a UV-Vis spectrometer (Shimadzu UV-2600). Hitachi F-4600 was used to measure the PL spectra. All the measurements were carried out in ambient air at room temperature.

The current density-voltage (*J-V*), luminance-voltage (*L-V*) and current efficiency-voltage (*CE-V*) relationships of PeLEDs were measured by a light-emitting diode testing system, including a computer connected Keithley 2400, a calculated Si photodiode (Photoelectric Instrument Factory of Beijing Normal University, ST-86LA). The EL spectra and the CIE color coordinates were collected by a PR670 spectrophotometer.

3 Results and discussion

The quality of the perovskite films is very important to the EL performance of the PeLEDs. Two films of ITO/PEDOT:PSS/10 wt.% $CsPbBr_3$ (Film A) and ITO/PEDOT:PSS/mCP/10 wt.% $CsPbBr_3$ (Film B) were prepared to study the effect of the mCP underlayer on the morphology, the structure, the UV-Vis absorption and photoluminescent (PL) properties of the perovskite films. The top-SEM images of Films A and B are shown in Fig. 1 (a) and (b), respectively. The $CsPbBr_3$ particles of Film B (with mCP) are smaller and more compact compared to Film A (without mCP). This plays a positive role in harvesting excitons, since the diffusion length is shorter in smaller perovskite grains. Meanwhile, the higher coverage will reduce the current leakage in the PeLEDs, and thus make the carrier be utilized more effectively.

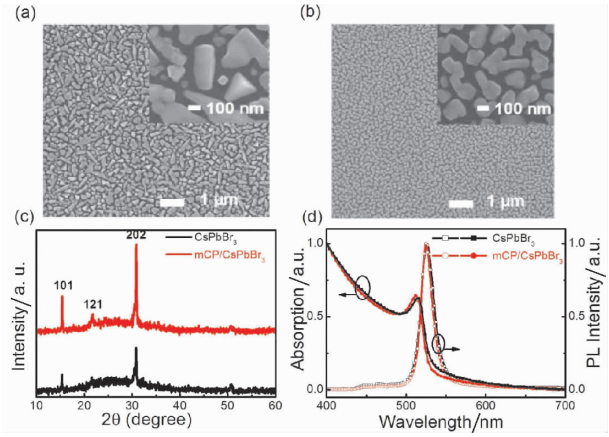

Fig. 1 The top-SEM images of (a) Film A and (b) Film B, (c) The XRD diffraction patterns and (d) UV-Vis and PL spectra of Films A and B.

In Fig. 1 (c), the two films exhibit similar XRD patterns with two diffraction peaks at 15.4° and 30.9° for both films. Besides this, there is an additional peak at 21.8° for Film B with an mCP underlayer. And all the intensities of the diffraction peaks of Film B are higher than those of Film A. It is reported that the diffraction peaks near 15.4°, 21.8° and 30.5° are corresponding to the (101), (121) and (202) planes of 10 wt.% $CsPbBr_3$, respectively[27]. These suggest that an orthorhombic crystal structure is formed for both perovskite films. The enhanced diffraction intensity of the perovskite with an mCP underlayer indicates that mCP is beneficial in forming a preferred orientation of the $CsPbBr_3$ film.

Fig. 1(d) exhibits the UV-Vis absorption spectra and photoluminescence (PL) spectra. Similar absorption spectra and PL spectra shapes are found in both films. However, both the absorption spectra peak (512 nm) and the PL spectra peak (525 nm) of Film B (with mCP) show a slight blue shift, compared to the absorption peak (515 nm) and the PL peak (526 nm) of Film A (without mCP), respectively. These suggest that the size of the perovskite

particles with the mCP underlayer is reduced according to the quantum size effect[28-29], which is consistent with the observations from the top-SEM images.

To investigate the role of mCP in the hole injection and transporting behavior of the devices, two hole dominated devices with the structure of: ITO (120 nm)/ PEDOT:PSS (30 nm) / *X* / TAPC (15 nm) / Al (120 nm), where *X* stands for without mCP (Device HDD1) and with mCP (Device HDD2). In Fig. 2, the current density of Device HDD2 with mCP is much larger than that of Device HDD1 at each applied voltage. It indicates that the mCP layer plays a significant role in improving the hole injection and transporting ability, which may also have a good effect on improving the EL performance of PeLEDs.

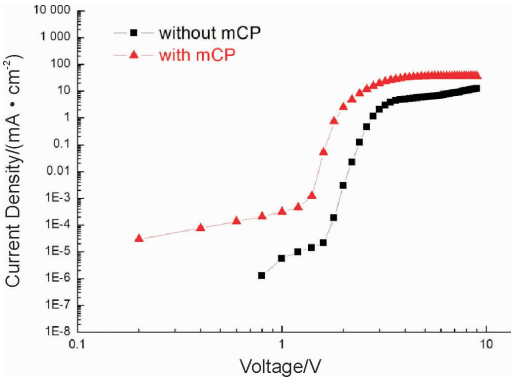

Fig. 2　The current density-voltage (*J-V*) curves of the hole-dominated Devices HDD1 (without mCP) and HDD2 (with mCP).

In order to study the effect of mCP on the EL performance of PeLEDs, two PeLEDs have been fabricated with structures of ITO (120 nm) / PEDOT:PSS (30 nm) / *Y* / $CsPbBr_3$/ TmPyPB (65 nm) / Liq (2.5 nm) / Al (120 nm), where *Y* stands for without mCP (Device A-1) and with mCP (Device B-1). The schematic diagram of the PeLEDs can be found in Fig. 3 (a). ITO is used as an anode. PEDOT:PSS is used as the hole injection and transport layer due to its high conductivity and transparency. mCP is inserted between PEDOT:PSS and $CsPbBr_3$ as an interface barrier layer to avoid their direct contact and to prevent the exciton quenching at the interface of PEDOT:PSS/$CsPbBr_3$. The energy level alignment of the PeLEDs is shown in Fig. 3 (b). The energy level values of the corresponding materials are from Refs. [14-16, 25-26, 30]. Since the high lowest unoccupied molecular orbital (LUMO) level (-2.4 eV) of mCP is much higher than the conduction band edge of 10 wt.% $CsPbBr_3$ (-3.35 eV), the electrons can be effectively confined on the VB of the $CsPbBr_3$ emitting layer. And the holes can be injected into the VB of $CsPbBr_3$ (-5.85 eV) via the HOMO of -5.90 eV of mCP. Thus, the exciton can be generated fully between the CB and VB in the $CsPbBr_3$, and harvest via light emitting more efficiently. The hole should be injected from PEDOT:PSS to mCP, and then across mCP and into $CsPbBr_3$ since the HOMO of mCP -5.90 eV[27] is almost the same to the valance band (VB) of $CsPbBr_3$ (-5.85 eV). Thus, the electrons and holes can be blocked and confined efficiently in $CsPbBr_3$. and forming into excitons efficiently in $CsPbBr_3$. Since the energy gap (E_g) of mCP is 3.5 eV, which is much larger than that of $CsPbBr_3$ (2.5 eV), the excitons can be confined better in $CsPbBr_3$ in the mCP based PeLEDs than in the ones without mCP.

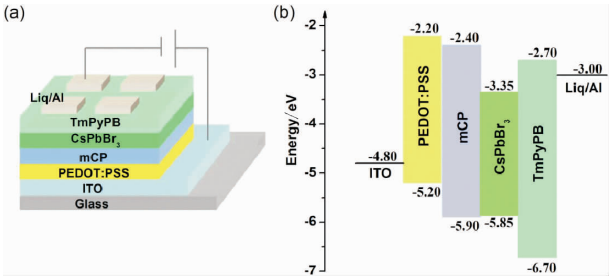

Fig. 3　(a) The schematic structure and (b) the energy level alignment of the PeLEDs

The current density-voltage (*J-V*) relationship, luminance-voltage (*L-V*) relationship, current efficiency-voltage-external quantum efficiency (*CE-V-EQE*) relationship and normalized EL spectra of the Devices A-1 and B-1, are shown in Fig. 4 (a) ~ (d). The detailed EL characteristics data of the Devices A-1 and B-1 is shown in Table 1. It was observed that the current density of Device B-1 (with mCP) is larger than that of Device A-1 (without

mCP) at each applied voltage. The turn on voltage decreases from 3.6 V (Device A-1) to 3.2 V (Device B-1). This can be attributed to the enhanced hole injection and transporting ability by the mCP interface barrier layer, which is demonstrated by the hole dominated devices. The luminance, current efficiency and external quantum efficiency are significantly improved. The maximum luminance (14 247 cd/m^2), the maximum CE (4.86 cd/A), the maximum EQE (1.26%) of Device B-1 are about 3.73, 4.22, and 4.20 folds to that (3 817 cd/m^2, 1.15 cd/A and 0.30%) of Device A-1, respectively. The normalized EL spectra of the two PeLEDs at 5 V are shown in Fig. 4 (d). The two PeLEDs exhibit high color-purity green-light without sub emission peak. The emission peak is located at 521 nm. The full width at half maxima (FWHM) is only 16 nm. This indicates that the EL spectra of the two PeLEDs are all from the intrinsic emission of $CsPbBr_3$.

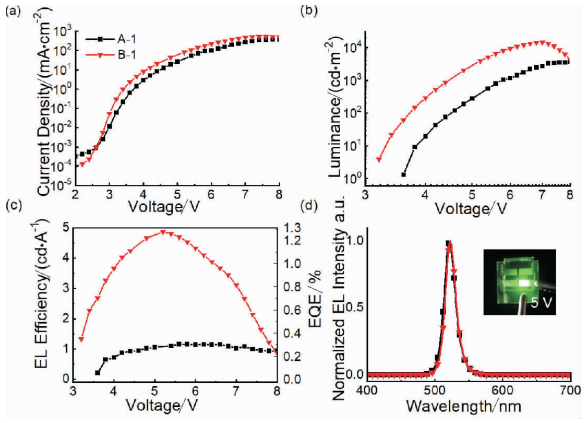

Fig. 4 EL performance of devices A-1 and B-1: (a) current density-voltage (*J-V*), (b) luminance-voltage (*L-V*), (c) current efficiency-voltage-external quantum efficiency (*CE-V-EQE*), (d) normalized EL spectra at 5 V. The inset of (d) is the emission photograph of the Device B-1 at 5 V

Table 1 The detailed EL characteristics data of the Devices A-1 and B-1

Devices	C^a/(mg · mL^{-1})	V_{on}^b/V	L_{max}^c/(cd · m^{-2})	CE_{max}^d/(cd · A^{-1})	EQE_{max}^e/%	FWHM^f/nm
A-1	0	3.6	3 817	1.15	0.30	16
B-1	8	3.2	14 247	4.86	1.26	16

Note: [a] The concentration of mCP in chlorobenzene, [b] The voltage at 1 cd/m^2, [c] The maximum luminance, [d] The maximum current efficiency, [e] The maximum external quantum efficiency, [f] The full width at half maxima at 5 V.

Fig. 5 exhibits the half lifetime of Devices A-1 and B-1, which were operated continuously at a constant voltage. The half lifetime (T_{50}) is defined as the time duration from the initial luminance (L_0) of the PeLEDs to the half intensity of the L_0. In our work, the L_0 is 100 cd/m^2. The half lifetime of Device B (27.8 s) is about 5.7 fold to that of Device A (4.9 s). It suggests the EL stability of the PeLEDs can be improved by inserting a mCP interface barrier layer between PEDOT:PSS and $CsPbBr_3$.

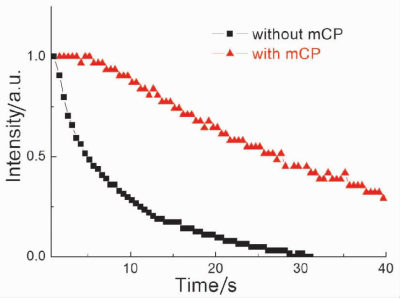

Fig. 5 The EL lifetime of the Devices A-1 (without mCP) and B-1 (with mCP)

The improved EL performance and stability of Device B-1 can be ascribed to three main reasons. Firstly, a higher quality $CsPbBr_3$ film with smaller grains, higher coverage and a preferred orientation of the $CsPbBr_3$ film can be achieved without changing the orthorhombic crystallization structure and the high purity color property. Smaller perovskite grains can reduce the diffusion length of the excitons, and thus promote the radiative recombination. Thus, the non-radiative recombination decay paths of excitons is reduced. Secondly, excitons can be generated in $CsPbBr_3$ EML and confined better in it. The holes can be easily injected into VB of $CsPbBr_3$ (−5.85 eV) from HOMO of mCP (−5.90 eV) without an injection barrier. Thus, excitons can be generated well on $CsPbBr_3$. Meanwhile, the separation of the layers of PEDOT:PSS and $CsPbBr_3$ by the mCP interface barrier layer can prevent the excitons diffusing from the $CsPbBr_3$ emitting layer into the PEDOT:PSS layer

and confine excitons in the $CsPbBr_3$ EML better due to the larger E_g (3.5 eV) of mCP compared to that of PEDOT:PSS (3 eV). Thirdly, the hole injection and transporting abilities are boosted and more excitons can be formed and utilized in the perovskite layer.

Thus, in Device A-1, significant exciton quenching and trap assisted charge recombination will be caused at the PEDOT:PSS/$CsPbBr_3$ interface due to the long exciton diffusion length of the excitons of $CsPbBr_3$ and the ionic transportation properties of PEDOT:PSS. While in Device B-1 with an mCP interface barrier layer between PEDOT:PSS and $CsPbBr_3$, exciton quenching will be largely reduced due to avoided direct contact of PEDOT:PSS and $CsPbBr_3$ and the remarkably reduced exciton diffusion from $CsPbBr_3$ to PEDOT:PSS. Meanwhile, the hole transport ability in PeLEDs is enhanced due to the good hole transport property of mCP. So the EL performance of Device B-1 is significantly improved.

To verify that the mCP interface barrier layer is feasible in different perovskite emitters, the quasi-2D $PEA_2Cs_{n-1}Pb_nBr_{3n+1}$ PeLEDs was fabricated with structure of ITO (120 nm) / PEDOT:PSS (30 nm) / *Z* / $PEA_2Cs_{n-1}Pb_nBr_{3n+1}$ / TmPyPB (65 nm) / Liq (2.5 nm) / Al (120 nm), where *Z* stands for without mCP (Device A-2) and with mCP (Device B-2). The *J-V* relationship, *L-V* relationship, *CE-V-EQE* relationship, and normalized EL spectra of the PeLEDs are shown in Fig. 6 (a) ~ (d). The detailed EL characteristics data of the Devices A-2 and B-2 are exhibited in Table 2. It was observed that the current density of Device B-2 (with mCP) is larger than that of Device A-2 (without mCP) at each applied voltage. It indicates that the carrier injection and transporting property can be enhanced by the mCP. The turn on voltage decreases from 3.6 V (Device A-2) to 3.3 V (Device B-2), which further indicates that the carrier injection and transporting efficiency can be increased by introducing the mCP. The luminance, current efficiency and external quantum efficiency are significantly improved. The maximum luminance (28 438 cd/m^2), the maximum CE (24.79 cd/A), the maximum EQE (6.52%) are about 1.63, 3.40, and 3.40 fold to that (17 406 cd/m^2, 7.28 cd/A and 1.92%) of Device A-2, respectively. And the same pure green color can be found in both PeLEDs with a peak wavelength around 521 nm and an FWHM of 16 nm at 5 V in Fig. 6(d) and Table 2.

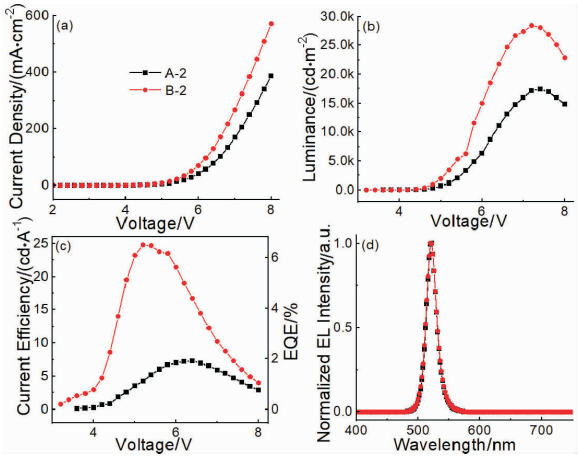

Fig. 6　EL performance of devices A-2 and B-2: (a) current density-voltage (*J-V*), (b) luminance-voltage (*L-V*), (c) current efficiency-voltage-external quantum efficiency-voltag (*CE-V-EQE*), (d) the normalized EL spectra at 5 V

Table 2　The detailed EL characteristics data of the Devices A-2 and B-2

Devices	C/(mg · mL^{-1})	V_{on}/V	L_{max}/(cd · m^{-2})	CE_{max}/(cd · A^{-1})	EQE_{max}/%	FWHM/nm
A-2	0	3.6	17 406	7.28	1.92	16
B-2	8	3.3	28 438	24.79	6.52	16

4　Conclusion

In this work, a very simple but effective interface barrier layer method has been developed. A small organic molecular mCP interface barrier layer was inserted between the perovskite EML and the hole injection and transport layer PEDOT:PSS by the

spincoating method. The EL performance of the mCP based $CsPbBr_3$ PeLEDs are significantly improved with the maximum EQE increased from 0.13% to 1.26%. Three reasons should be counted into it. Firstly, the film quality is largely improved with smaller grains, higher coverage and a preferred orientation of the $CsPbBr_3$ film. Secondly, excitons will be mostly generated on $CsPbBr_3$ and confined in the $CsPbBr_3$ EML due to larger E_g of mCP and suitable energy alignment of HOMO of mCP and VB of $CsPbBr_3$. Thirdly, the hole injection and transporting abilities are boosted and more excitons can be formed and utilized in the perovskite layer. Thus, the non-radiative recombination decay paths of excitons is reduced, leading to an enhancement in EL performance of the mCP basd $CsPbBr_3$ PeLEDs. Further, this method was verified in the quasi-2D PeLEDs. The application of mCP as an interface barrier layer and exciton confine layer in both the 3D and quasi-2D PeLEDs greatly improves the EL performance of PeLEDs. And the fabrication process is simple and reliable. It provides a feasible method for further research on PeLEDs aiming at high performance and low cost.

References:

[1] Tan Z K, Moghaddam R S, Lai M L, et al. Bright light-emitting diodes based on organometal halide perovskite[J]. Nature Nanotechnology, 2014, 9(9):687-692.

[2] Lin K B, Xing J, Quan L N, et al. Perovskite light-emitting diodes with external quantum efficiency exceeding 20 per cent [J]. Nature, 2018, 562(7726):245-248.

[3] Kim Y H, Kim S, Kakekhani A, et al. Comprehensive defect suppression in perovskite nanocrystals for high-efficiency light-emitting diodes[J]. Nature Photonics, 2021, 15(2):148-155.

[4] Li X, Gao X P, Zhang X T, et al. Lead-free halide perovskites for light emission: Recent advances and perspectives[J]. Advanced Science, 2021, 8(4):2003334.

[5] Kim J S, Heo J M, Park G S, et al. Ultra-bright, efficient and stable perovskite light-emitting diodes[J]. Nature, 2022, 611(7937):688-694.

[6] Li M L, Zhao Y P, Qin X Q, et al. Conductive phosphine oxide passivator enables efficient perovskite light-emitting diodes [J]. Nano Letters, 2022, 22(6):2490-2496.

[7] Xia Y, Li Y H, Wang Z K, et al. Domain distribution management of quasi-2D perovskites toward high-performance blue light-emitting diodes[J]. Advanced Functional Materials,2023,33(35):2303423.

[8] Bai W H, Xuan T, Zhao H Y, et al. Perovskite light-emitting diodes with an external quantum efficiency exceeding 30% [J]. Advanced Materials,2023, 35(39):2302283.

[9] Abdi-Jalebi M, Andaji-Garmaroudi Z, Cacovich S, et al. Maximizing and stabilizing luminescence from halide perovskites with potassium passivation[J]. Nature, 2018, 555(7697):497-501.

[10] Huang H, Raith J, Kershaw S V, et al. Growth mechanism of strongly emitting $CH_3NH_3PbBr_3$ perovskite nanocrystals with a tunable bandgap[J]. Nature Communications, 2017, 8(1):996.

[11] Wang H R, Zhang X Y, Wu Q Q, et al. Trifluoroacetate induced small-grained $CsPbBr_3$ perovskite films result in efficient and stable light-emitting devices[J]. Nature Communications, 2019, 10(1):665.

[12] Stranks S D, Eperon G E, Grancini G, et al. Electron-hole diffusion lengths exceeding 1 micrometer in an organometal trihalide perovskite absorber[J]. Science, 2013, 342 (6156):341-344.

[13] Lu B, Yuk H, Lin S, et al. Pure PEDOT:PSS hydrogels[J]. Nature Communications, 2019, 10(1):1043.

[14] Yu F X, Zhang Y, Xiong Z Y, et al. Full coverage all-inorganic cesium lead halide perovskite film for high efficiency light-emitting diodes assisted by 1,3,5-tri(m-pyrid-3-yl-phenyl)benzene[J]. Organic Electronics, 2017, 50:480-484.

[15] Wang R, Jia Y L, Ding L, et al. Efficient halide perovskite light-emitting diodes with emissive layer consisted of multilayer coatings[J]. Journal of Applied Physics, 2019, 126(16):165502.

[16] Ravi V K, Markad G B, Nag A. Band edge energies and excitonic transition probabilities of colloidal $CsPbX_3$ (X = Cl, Br, I) Perovskite Nanocrystals[J]. ACS Energy Letters, 2016, 1(4):665-671.

[17] Kim Y H, Cho H, Heo J H, et al. Multicolored organic/inorganic hybrid perovskite light-emitting diodes[J]. Advanced Materials, 2015, 27(7):1248-1254.

[18] Peng X F, Wu X Y, Ji X X, et al. Modified conducting polymer hole injection layer for high-efficiency perovskite light-emitting devices: Enhanced hole injection and reduced luminescence quenching[J]. The Journal of Physical Chemistry Letters, 2017, 8(19):4691-4697.

[19] Tsai T C, Chang H C, Chen C H, et al. A facile dedoping approach for effectively tuning thermoelectricity and acidity of pedot: PSS films[J]. Organic Electronics, 2014, 15(3):641-645.

[20] Wang Q, Chueh C C, Eslamian M, et al. Modulation of pedot: PSS pH for efficient inverted perovskite solar cells with reduced potential loss and enhanced stability[J]. ACS Applied Materials & Interfaces, 2016, 8(46):32068-32076.

[21] Meng Y, Ahmadi M, Wu X Y, et al. High performance and stable all-inorganic perovskite light emitting diodes by reducing luminescence quenching at PEDOT:PSS/perovskites interface[J]. Organic Electronics, 2019, 64:47-53.

[22] Lin C Y, Chen P, Xiong Z Y, et al. Interfacial engineering with ultrathin poly (9,9-di-n-octylfluorenyl-2,7-diyl) (PFO) layer for high efficient perovskite light-emitting diodes[J]. Nanotechnology, 2018, 29(7):075203.

[23] Zou Y T, Ban M Y, Yang Y G, et al. Boosting perovskite light-emitting diode performance via tailoring interfacial contact [J]. ACS Applied Materials & Interfaces, 2018, 10(28):24320-24326.

[24] Zhao Y P, Li M L, Qin X Q, et al. Efficient perovskite light-emitting diodes by buried interface modification with triphenylphosphine oxide[J]. ACS Applied Materials & Interfaces, 2023,15(2):3644-3650.

[25] Wang R, Jia Y L, Zhang Y, et al. High efficiency green perovskite light-emitting diodes based on exciton blocking layer [J]. Acta Physica Sinica, 2020, 69(3):038501.

[26] Cui L S, Liu Y, Yuan X D, et al. Bipolar host materials for high efficiency phosphorescent organic light emitting diodes: Tuning the HOMO/LUMO levels without reducing the triplet energy in a linear system[J]. Journal of Materials Chemistry C, 2013, 1(48):8177-8185.

[27] Ling Y C, Tian Y, Wang X, et al. Enhanced optical and electrical properties of polymer-assisted all-inorganic perovskites for light-emitting diodes[J]. Advanced Materials, 2016, 28(40):8983-8989.

[28] Wu T, Yang Y G, Zou Y T, et al. Nanoplatelet modulation in 2d/3d perovskite targeting efficient light-emitting diodes[J]. Nanoscale, 2018, 10(41):19322-19329.

[29] Kim Y H, Wolf C, Kim Y T, et al. Highly efficient light-emitting diodes of colloidal metal-halide perovskite nanocrystals beyond quantum size[J]. ACS Nano, 2017, 11(7):6586-6593.

[30] Mu H C, Jiang Y X, Xie H F. Efficient blue phosphorescent organic light emitting diodes based on exciplex and ultrathin FIrpic sandwiched layer[J]. Organic Electronics, 2019, 66:195-205.

【责任编辑: 卓祯雨】